Analytical Methods

ROYAL SOCIETY OF CHEMISTRY

PAPER

View Article Online
View Journal

Cite this: DOI: 10.1039/d1ay00129a

Development of nanobody-based flow-through dot ELISA and lateral-flow immunoassay for rapid detection of 3-phenoxybenzoic acid†

Can Zhang, *[ab] Xiaoxiao Wu,[a] Dongyang Li,[b] Jinnuo Hu,[a] Debin Wan,[b] Zhen Zhang[c] and Bruce D. Hammock [b]

Received 23rd January 2021
Accepted 3rd March 2021

DOI: 10.1039/d1ay00129a

rsc.li/methods

As a major metabolite of pyrethroid pesticides, 3-phenoxybenzoic acid (3-PBA) can be an indicator of health risk and human exposure assessment. Based on nanobodies (Nbs), we have developed a rapid flow-through dot enzyme linked immunosorbent assay (dot ELISA) and gold nanoparticle (GNP) lateral-flow immunoassay for detecting 3-PBA. The limit of detection (LOD) values for detecting 3-PBA by flow-through dot ELISA and GNP lateral-flow immunoassay were 0.01 ng mL^{-1} and 0.1 ng mL^{-1}, respectively. The samples (urine and lake water) with and without 3-PBA were detected by both nanobody-based flow-through dot ELISA and GNP lateral-flow immunoassay, as well as liquid chromatography-mass spectrometry (LC-MS) for validation. There was good consistency between the results of the immunoassays. This demonstrated that the two developed nanobody-based immunoassays are suitable for rapid detection of 3-PBA.

1. Introduction

3-PBA is a common metabolite of a class of pyrethroid pesticides, such as fenpropathrin, cyhalothrin, flucythrinate, and permethrin, and can be used as a criterion of exposure assessment in the environment.[1–3] Compared with pyrethroid compounds, it is regarded relatively non-toxic. However, people may unconsciously ingest food contaminated with pyrethroids.[4,5] Besides, people may also get exposed to 3-PBA through environmental media such as water. Research showed that 3-PBA mainly exists in human urine and blood, and its effect on estrogen can cause endocrine metabolism disorder.[6] Therefore, people pay more attention to monitoring and assessment of 3-PBA.

Some methods have been established to detect 3-PBA, including instrumental analysis methods (*e.g.* high-performance liquid chromatography,[7,8] supercritical fluid chromatography,[9] gas chromatography-mass spectrometry[10–13]) and immunoassays (*e.g.* enzyme immunoassay,[14–17] electrochemical immunoassay,[18,19] fluorescence immunoassay[20,21]). Instrumental methods are of high sensitivity and easy to automate. However, the cost is high and the sample's clean-up is complex and time-consuming. Traditional ELISA, especially membrane-based immunoassay, is suitable for high-throughput screening because of its sensitivity and visual evaluation.[22] For the establishment of sensitive membrane-based immunoassays, the selection of antibodies plays a key role.

In the past, most of the antibodies (Abs) used for detecting 3-PBA were monoclonal antibodies (mAbs) and polyclonal antibodies (pAbs).[23–25] Liu *et al.* established a membrane-based immunoassay which used colloidal gold labeled mAbs for detecting 3-PBA in river water and the LOD value was 1 μg mL^{-1}.[26] As genetic engineering techniques developed, various small size Abs have been found. A new subclass of Abs in members of the camelid family was discovered and called heavy-chain Abs.[27] Recombinant expression of the heavy chain variable domains yields antibodies known as nanobodies (Nbs).[28] Compared with traditional Abs (pAbs and mAbs), Nbs have many advantages, including thermostability, accessibility and strong specificity.[29,30] With the extensive development of Nbs, Nbs were gradually applied in the field of detection, such as pathogen diagnosis and pollutant detection.[31,32] Kim[14] *et al.* first isolated VHH establishing VELISA for detecting 3-PBA, and the half-maximal inhibitory concentration (IC_{50}) could reach 1.4 ng mL^{-1} after the fifth round of panning. To improve the sensitivity of 3-PBA detection, Huo[17] *et al.* used nanobody–alkaline phosphatase fusion protein to develop a direct competitive fluorescence enzyme immunoassay (dc-FEIA), which achieved a LOD of 0.011 ng mL^{-1}. Sun *et al.* established a nanobody-based competitive dot ELISA for visual

[a]School of Food & Biological Engineering, Jiangsu University, Zhenjiang 212013, China. E-mail: zhangcan@mail.ujs.edu.cn; Tel: +86 0511 88780201

[b]Department of Entomology and Nematology and UCD Comprehensive Cancer Center, University of California, Davis, California 95616, USA

[c]School of the Environment and Safety Engineering, Jiangsu University, Zhenjiang, 212013, China

† Electronic supplementary information (ESI) available. See DOI: 10.1039/d1ay00129a

screening of ochratoxin A in cereals, and the cut-off level of this visualization assessment was 5 μg kg^{-1}.[33]

In this research, a nanobody-based flow-through dot enzyme linked immunosorbent assay (Nb-based flow-through dot ELISA) and gold nanoparticle-labeled nanobody lateral-flow immunoassay (GNP-Nb lateral-flow immunoassay), which used a nitrocellulose membrane as the supporter, were established for sensitive and rapid detection of 3-PBA. To verify the reliability of the rapid assays, healthy volunteers' urine and lake water were selected for analysis and the results were consistent with those of the LC-MS method. Due to the advantages of high sensitivity, rapid detection and low-cost, these developed membrane-based immunoassays using Nbs can be applied as effective and convenient screening tools for monitoring 3-PBA residues in a biological matrix or an environment matrix.

2. Materials and methods

2.1 Chemicals and reagents

3-PBA standard was purchased from Aladdin (Shanghai, China). Bovine serum albumin (BSA) was purchased from Sigma-Aldrich. Chloroauric acid ($HAuCl_4 \cdot 4H_2O$), trisodium citrate, Tween-20 and methanol were obtained from Sinopharm (Shanghai Sinopharm Group Chemical reagent Co., Ltd.). 6*his-tag monoclonal antibodies (McAbs) (Cat No. 66005-1-1g) and HRP-conjugated 6*his-tag McAbs (Cat No. HRP-66005) were purchased from Proteintech Group, Inc. 3,3′,5,5′-Tetramethylbenzidine (TMB) was purchased from Huinuo Biotechnology (Shenzhen, China). The coating antigen (3-PBA–BSA) and the *Escherichia coli* TOP10F′ strain used to express anti-3-PBA nanobodies containing a plasmid were provided by Hammock Lab.[14] After expression and purification, the concentration of the obtained anti-3-PBA Nbs was 0.3 mg mL^{-1}. Other chemicals were of analytical grade. Two types of nitrocellulose (NC) membranes were purchased from Merck Millipore Ltd (Cat No. HATF00010 and HF13502S25).

2.2 Nb-based flow-through dot ELISA

The pre-treatment of the NC membrane for flow-through dot ELISA was performed with slight modification as the reference described.[33] Briefly, slight marks were made at center areas to

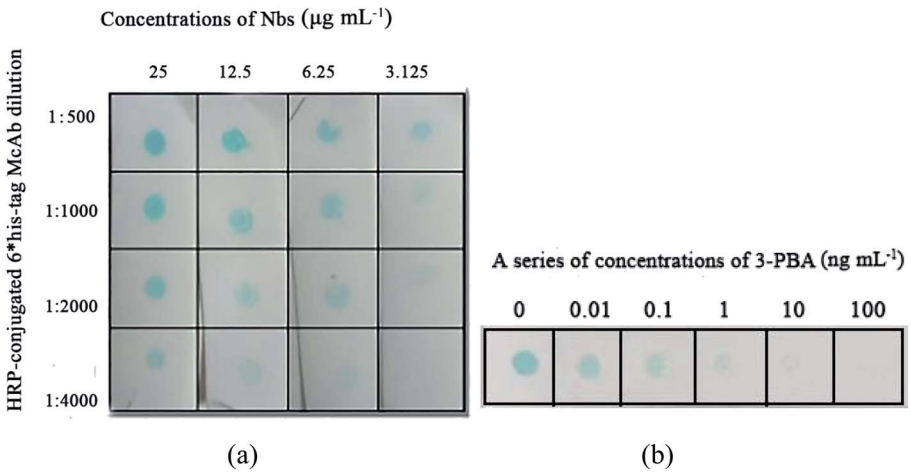

Fig. 1 Nb-based flow-through dot ELISA. (a) Optimization of Nbs and HRP-conjugated 6*his-tag McAbs; (b) a series of concentrations of 3-PBA detected by Nb-based flow-through dot ELISA.

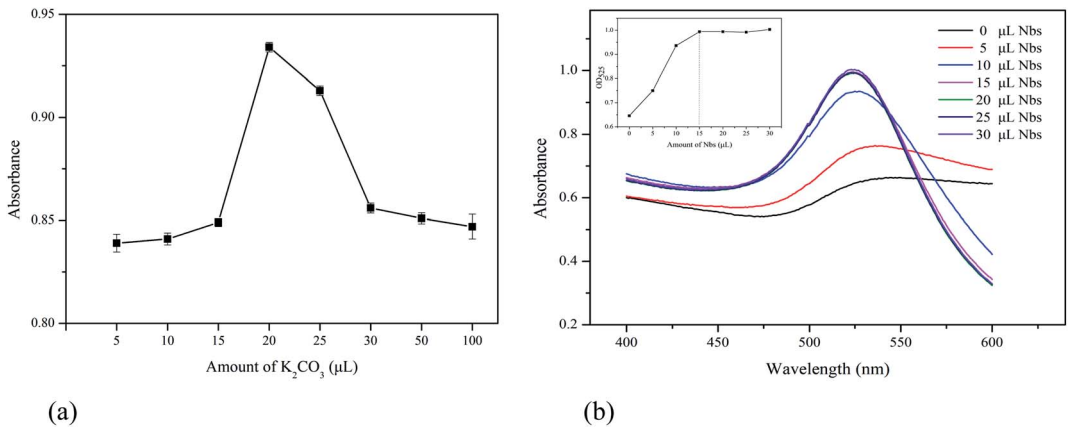

Fig. 2 Optimization of GNP labeling of Nbs. (a) Amount of K_2CO_3 ($n = 3$); (b) amount of Nbs.

locate the reaction zone on the membrane and the membrane was immersed in PBS buffer for activation. Five μL of coating antigen 3-PBA–BSA (75 μg mL^{-1}) was dropped onto the reaction zone. After the liquid flowed through, the membrane was blocked by immersing in PBS solution containing 3% non-powered milk (m/v) for 1 h. Finally, the membranes were washed, dried at room temperature, and stored at 4 °C until use.

Nb-based flow-through dot ELISA for 3-PBA detection was performed as per the following procedures: first, different concentrations of 3-PBA solution and anti-3-PBA Nbs were pre-mixed, and then dropped onto the reaction zone. After the liquid flowed through the membrane completely, the membrane was washed with PBST. Then 5 μL of 500-fold-diluted secondary antibodies (HRP-conjugated 6*his-tag McAbs) was added. Finally, the NC membrane was immersed in a TMB substrate solution for coloration. After 10 min, the color of each dot was visually judged by comparing with the negative control (without 3-PBA).

2.3 Gold nanoparticle labeled Nbs (GNP-Nbs)

Gold nanoparticles (GNPs) with a diameter of about 20 nm were prepared according to the procedure described by Frens.[34] Briefly, l00 mL of 0.01% $HAuCl_4$ solution (in Milli-Q purified water) was boiled thoroughly. Then 1% trisodium citrate solution was added under constant stirring. The generated GNP colloidal solution was cooled to room temperature and stored at 4 °C until use.

For protein labeling of GNPs, a protein has the best adsorption capacity when the pH value is close to its isoelectric point (pH ≥ pI).[35] The pH of GNPs was adjusted by adding different amounts of K_2CO_3. For 1 mL GNP solution, different volumes (5, 10, 15, 20, 25, 30, 50 and 100 μL) of 0.2 mol L^{-1} K_2CO_3 were separately added to adjust the pH value. Excess Nbs were added to the GNP solution containing different amounts of K_2CO_3 and incubated for 1 h. Then to each tube was added 50 μL of 10% NaCl and left standing for 30 min before scanning under 400–600 nm. The amount of K_2CO_3 corresponding to the value at λ_{max} was chosen for the regulation of GNP solution before coupling with Nbs. The procedure was performed three times repeatedly. Once the optimal pH conditions were set, different amounts of 0.3 mg mL^{-1} Nbs (5, 10, 15, 20, 25 and 30 μL) were also optimized according to the same procedure. GNP-Nbs were centrifuged for 30 min at 10 000 rpm, and the sediment was dissolved

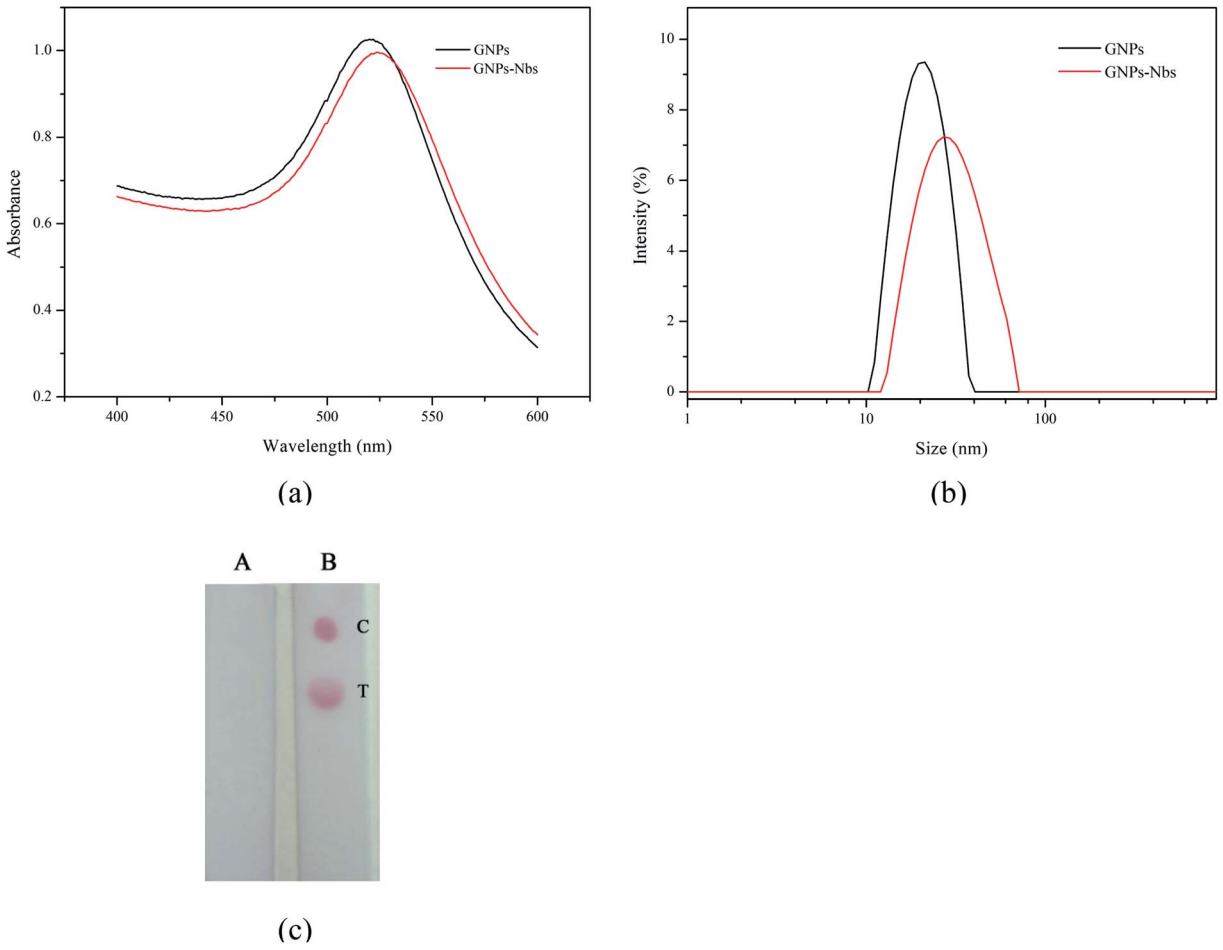

Fig. 3 Verification of GNP-Nbs. (a) Scanning spectra of GNPs and GNP-Nbs; (b) particle size analysis of GNPs and GNP-Nbs; (c) verification of GNP-Nbs by lateral-flow immunoassay: GNPs (A); GNP-Nbs (B).

with storage buffer (containing 1% BSA and 0.25% Tween-20).

2.4 GNP-Nb lateral-flow immunoassay

The NC membrane for the GNP-Nb lateral-flow immunoassay was prepared according to the study reported by Zhang.[36] One microliter of 50 μg mL^{-1} 3-PBA–BSA was coated as the test zone and 1 μL of 6*his-tag McAbs (20-fold diluted) was coated as the control zone. The mixed solution containing GNP-Nbs (10-fold diluted) and different concentrations of 3-PBA was dropped onto the edge of the membrane until the liquid migrated across the test zone and the control zone completely.

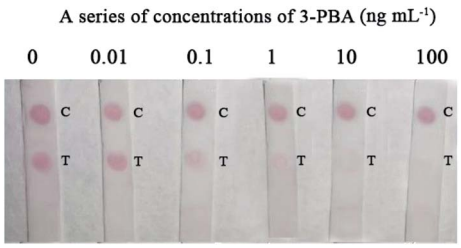

Fig. 4 A series of concentrations of 3-PBA detected by GNP-Nb based lateral-flow immunoassay.

2.5 Cross-reactivity

To assess the specificity of the competitive immunoassays, cross-reactivity (CR) of anti-3-PBA Nbs with structural analogues (3-phenoxybenzaldehyde, 3-phenoxybenzyl alcohol and 4-(3-hydroxyphenoxy)benzoic acid) was also determined by Nb-based flow-through dot ELISA and GNP-Nb lateral-flow immunoassay.

2.6 Matrix effect and sample analysis

To evaluate the matrix effect, a series of concentrations of 3-PBA were prepared in 10% methanol/PBS (as the standard) and a negative sample matrix. They were measured using plate ELISA, flow-through dot ELISA and lateral-flow immunoassay. To facilitate the quantitative analysis of flow-through dot ELISA and lateral-flow immunoassay, we also used Adobe Photoshop CC software to analyze the images of the standard solution and calculated the inhibition ratio by comparing the grayscale difference of the dot's color to get the standard curve.

We took urine samples from healthy volunteers and lake water from Jiangsu University with no exposure to pyrethroid insecticides for spiking analysis. Urine collection was performed following the guidelines and protocols of the Jiangsu University. The samples were proved to be free of 3-PBA by LC-MS analysis. The urine samples were centrifuged at 10 000 rpm for 10 min, and the supernatant was filtered using a 0.22 μm

Table 1 Cross-reactivity detected by Nb-based flow-through dot ELISA, GNP-Nb lateral-flow immunoassay and plate ELISA

		Cross-reactivity		
Analytes	Chemical structures	Flow-through dot ELISA	Lateral-flow immunoassay	Plate ELISA
3-Phenoxybenzoic acid	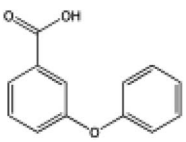	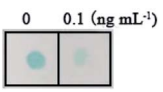	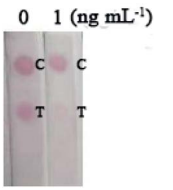	100%
3-Phenoxybenzaldehyde	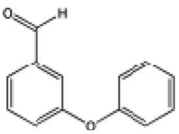	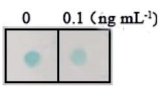	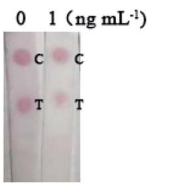	75.1%
4-(3-Hydroxyphenoxy)benzoic acid	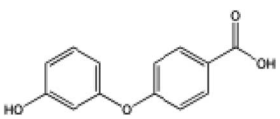	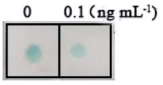	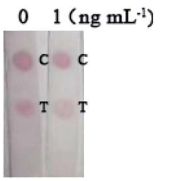	13.5%
3-Phenoxybenzyl alcohol	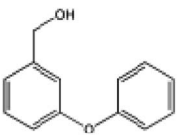	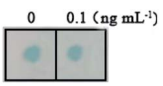	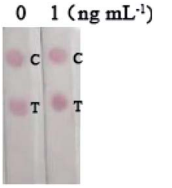	<0.1%

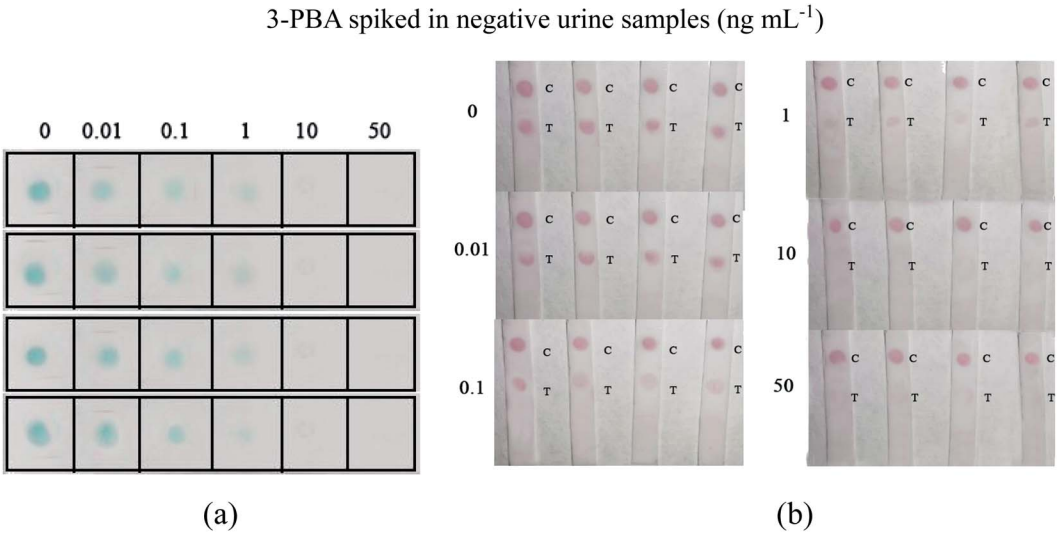

Fig. 5 Spiked sample analysis ($n = 4$). (a) Nb-based flow-through dot ELISA; (b) GNP-Nb lateral-flow immunoassay.

filter membrane before immunoassays. The lake water was directly analyzed after filtration. Sample treatment for LC-MS analysis was the same as described by Huo.[17]

Negative samples confirmed to be free of 3-PBA by LC-MS were spiked with 3-PBA at concentrations of 0.1, 1, 10, and 50 ng mL^{-1} for recovery analysis. The recovery analysis was done repeatedly four times. We also used software to quantitatively analyze the images of the visual results, and validated them by LC-MS to get the correlation. Negative samples were also randomly spiked with 3-PBA and simultaneously analyzed using Nb-based flow-through dot ELISA, GNP-Nb lateral-flow immunoassays and LC-MS.

3. Results and discussion

3.1 Nb-based flow-through dot ELISA

To get better visual judgement, we first performed the optimization of experimental parameters. The concentrations of Nbs and HRP-conjugated 6*his-tag McAbs were optimized by checkerboard titration (Fig. 1a). The color of the dot faded down as the concentration of Nbs decreased from 25 μg mL^{-1} to 3.125 μg mL^{-1}. When the dilution of HRP-conjugated 6*his-tag McAbs increased, the dot color became weak. For flow-through dot ELISA, Nbs at a concentration of 25 μg mL^{-1} and 500-fold diluted HRP-conjugated 6*his-tag McAbs were applied for the following analysis. A series of concentrations of 3-PBA were added for the competitive immunoassay. In this method, the reaction is a competitive combination of the coating antigen and free 3-PBA with Nbs. When the concentration of free 3-PBA was too high, Nbs could combine with it completely in the mixture. There were no excess Nbs to combine with the coating antigen on the membrane, so the test zone was colorless. The intensity of the dot's color was inversely proportional to the concentration of 3-PBA. When the concentration of 3-PBA reached 0.01 ng mL^{-1} (Fig. 1b), the dot color could still be distinguished from the negative control (without 3-PBA), which was defined as the cutoff value for Nb-based flow-through dot ELISA.

3.2 Optimization of gold nanoparticle labeled Nbs

In the process of labeling, the pH value played a key role. The pH value of the GNP solution was adjusted by adding different amounts of K_2CO_3. Fig. 2a shows the pH effect on labeling, and along with the increase of K_2CO_3 volume from 0 to 100 μL, the absorbance at λ_{max} increased, reaching a maximum value at 20

Table 2 Spiked negative samples detected by Nb-based flow-through dot ELISA, GNP-Nb lateral-flow immunoassay and LC-MS ($n = 4$)[a]

	Visual results[b]			
3-PBA spiked (ng mL^{-1})	Flow-through dot ELISA	Lateral-flow immunoassay	LC-MS[c] (ng mL^{-1})	LC-MS recovery (%)
0.1	+, +, +, +	−/+, +, −/+, +	0.097 ± 0.070	97
1	+, +, +, +	+, +, +, +	0.981 ± 0.045	98
10	+, +, +, +	+, +, +, +	10.3 ± 0.8	103
50	+, +, +, +	+, +, +, +	50.7 ± 2.6	101

[a] +: positive, the dot color is weaker than that of the control; −: negative, the dot color is brighter than that of the control; −/+: negative/positive, the dot color is similar to that of the control. [b] Qualitative detection by Nb-based flow-through dot ELISA and GNP-Nb lateral-flow immunoassay. [c] Quantitative analysis by LC-MS.

Table 3 Randomly spiked samples analyzed by Nb-based flow-through dot ELISA, GNP-Nb lateral-flow immunoassay and LC-MS[a]

	Visual results ($n = 3$)			
Sample	Flow-through dot ELISA	Lateral-flow immunoassay	LC-MS (ng mL^{-1})	RSD (%)
U1	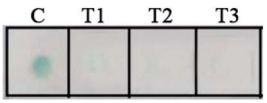	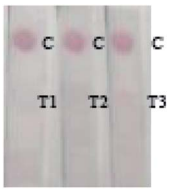	45.1 ± 1.1	2.4
U2	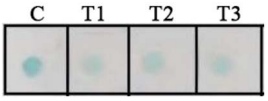	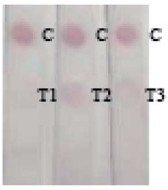	1.11 ± 0.07	6.3
U3	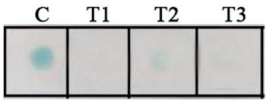	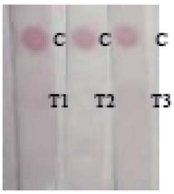	22.6 ± 0.5	2.2
U4	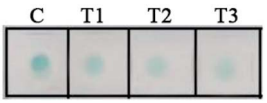	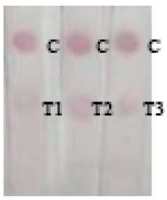	0.67 ± 0.04	5.9
L1	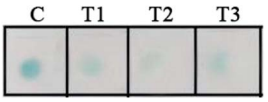	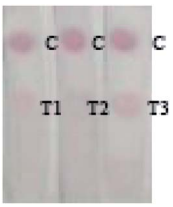	4.63 ± 0.26	5.6
L2	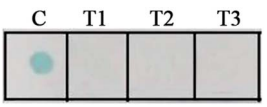	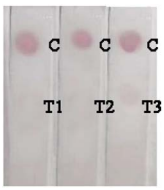	11.7 ± 0.8	6.8
L3	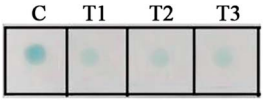	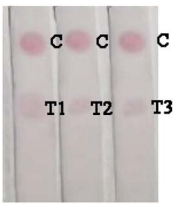	2.47 ± 0.12	4.8

Table 3 (*Contd.*)

Sample	Visual results ($n = 3$) Flow-through dot ELISA	Lateral-flow immunoassay	LC-MS (ng mL^{-1})	RSD (%)
L4	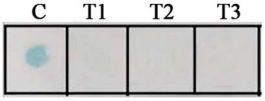	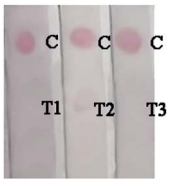	50.7 ± 1.6	3.2

[a] U and L: randomly spiked in urine (U) and lake water (L) samples, respectively; C: control; T1–T3: repeated sample detection.

μL K_2CO_3, and the conjugation between GNPs and Nbs reached the best stable state. With a gradual increase of the amount of Nbs (Fig. 2b) at the optimum pH, the maximum absorption peak and its corresponding absorbance almost remained constant and the optimal conjugation state was reached when the amount of Nbs was 15 μL (at a concentration of 0.3 mg mL^{-1}). Based on these parameters, for 1 mL GNP solution, the optimum labeling conditions were 20 μL K_2CO_3 (0.2 mol L^{-1}) for pH adjustment and 15 μL Nbs (0.3 mg mL^{-1}) for conjugation. The GNPs and GNP labeled Nbs were characterized by wavelength scanning from 400 to 600 nm. After conjugation, the λ_{max} of GNPs showed a redshift from 520 nm to 525 nm, which could preliminarily indicate successful conjugation (Fig. 3a). The characterization of GNPs and GNP-Nbs by transmission electron microscopy (TEM) and particle size analysis is shown in Fig. S1.† From the TEM images, it can be observed that both GNPs and GNP-Nbs are well-dispersed without aggregation. The particle size of GNP-Nbs reached 30 nm, while the size of bare GNPs was about 20 nm (Fig. 3b). To further verify the successful conjugation, both GNPs and GNP-Nbs were selected for lateral-flow immunoassay (Fig. 3c). GNPs did not form red spots on the NC membrane (Fig. 3c-A), and GNP-Nbs showed red spots which indicated specific binding between the coating antigen and GNP-Nbs (Fig. 3c-B) for successful conjugation.

3.3 GNP-Nb based lateral-flow immunoassay

Fig. 4 shows the competitive GNP-Nb lateral-flow immunoassay for 3-PBA detection. The Nbs first mixed with 3-PBA, and along with the increase in concentration of 3-PBA, the color of the test zone gradually faded. When the concentration of 3-PBA was more than 0.1 ng mL^{-1}, the color of the test zone could be easily distinguished from the color of the test zone without 3-PBA. Thus, the LOD of the GNP-Nb lateral-flow immunoassay was determined to be 0.1 ng mL^{-1}.

3.4 Cross-reactivity analyzed by Nb-based flow-through dot ELISA and GNP-Nb lateral-flow immunoassay

The Nb-based flow-through dot ELISA and GNP-Nb lateral-flow immunoassay were also applied for the detection of other structural analogues (3-phenoxybenzaldehyde, 3-phenoxybenzyl alcohol and 4-(3-hydroxyphenoxy)benzoic acid). The specificity and validation of the developed assays were studied. As shown in Table 1, the concentrations 0.1 ng mL^{-1} and 1 ng mL^{-1} were selected for cross-reactivity analysis. The analogues 3-phenoxybenzaldehyde and 4-(3-hydroxyphenoxy)benzoic acid showed cross-reactivities of 75.1% and 13.5% in plate ELISA, and 3-phenoxybenzyl alcohol showed no cross-reactivity with 3-PBA (<0.1%). The results also indicated that the higher cross-reactivity led to more similar detection images from Nb-based flow-through dot ELISA and GNP-Nb lateral-flow immunoassay.

3.5 Sample analysis

We studied the influence of negative urine and lake water as matrixes on Nb-based flow-through dot ELISA, GNP-Nb lateral-flow immunoassay and plate ELISA. A series of concentrations of 3-PBA were separately dissolved in 10% methanol/PBS and negative sample matrixes. The detection results of the three immunoassays were compared and they showed good consistency (Fig. S2†). For Nb-based flow-through dot ELISA and GNP-Nb lateral-flow immunoassay, the influence of the matrix almost can be ignored. The images were captured using a smartphone and analyzed with software, and the gray scale and standard curve of the two methods are shown in Fig. S3.† The cutoff levels, defined as the concentration corresponding to 10% inhibition ratio, were 0.01 ng mL^{-1} and 0.1 ng mL^{-1}, respectively. The results were also consistent with those of visual judgement results.

To evaluate the validation of Nb-based flow-through dot ELISA and GNP-Nb lateral-flow immunoassay, we spiked 3-PBA in negative urine samples at concentrations of 0.1, 1, 10, and 50 ng mL^{-1}. Fig. 5 shows that the dot color faded down when the spiked concentration increased. The recoveries by LC-MS ranged from 97% to 103% (Table 2). The quantitative analysis of the visual results is shown in Table S1.† And the correlation curves of flow-through dot ELISA ($R^2 = 0.982$) and GNP-Nb lateral-flow immunoassay ($R^2 = 0.973$) between LC-MS showed good consistency (Fig. S4†). We also used the data to obtain ROC curves, shown in ESI (Fig. S5).† The results showed that the

cut-off values of flow-through dot ELISA and lateral-flow immunoassay were 0.011 ng mL^{-1} and 0.107 ng mL^{-1}, which were consistent with the visual results. We also randomly spiked 3-PBA in negative samples and analyzed by Nb-based flow-through dot ELISA and GNP-Nb lateral-flow immunoassay (Table 3). The visual results obtained by flow-through dot ELISA (3-PBA > 0.1 ng mL^{-1}) showed good consistency with LC-MS results. As well, the results obtained by lateral-flow immunoassay (3-PBA > 0.1 ng mL^{-1}) showed good consistency with LC-MS results. Therefore, the developed Nb-based flow-through dot ELISA and GNP-Nb lateral-flow immunoassay demonstrated to be practical biological monitoring methods for rapid screening of 3-PBA.

4. Conclusion

We developed two formats (flow-through and lateral-flow) of rapid and convenient Nb-based immunoassays for 3-PBA detection. The results can be evaluated by the color change of the reaction zone which could be directly judged by the naked eye. The LOD value of GNP-Nb based lateral-flow immunoassay for 3-PBA detection was 0.1 ng mL^{-1}, which was 100-fold sensitive than the mAb-based lateral-flow immunoassay reported by Liu.[26] The flow-through dot ELISA was more sensitive, but the process of GNP-Nb lateral-flow immunoassay was more convenient because there was no step for substrate participation and the detection time is within 10 min. The spiked samples were tested by Nb-based flow-through dot ELISA and GNP-Nb lateral-flow immunoassay, which showed consistency with the results of LC-MS. As Nbs have the advantage of anti-matrix interference, samples can be analyzed without complicated treatments. Moreover, the membrane-based immunoassays (flow-through and lateral-flow) perform the operation more quickly than instrumental methods for high-throughput sample analysis. Therefore, Nb-based flow-through dot ELISA and GNP-Nb lateral-flow immunoassay are suitable for visual evaluation and qualitative on-site sensitive detection of 3-PBA in a biological matrix and an environmental matrix.

Ethical statement

All applicable procedures for the use of urines were approved by the Ethical Committee of Jiangsu University and performed following the guidelines and protocols of Jiangsu University.

Author contributions

Can Zhang: conceptualization, methodology, resources, writing – review & editing, supervision. Xiaoxiao Wu: methodology, formal analysis, investigation, data curation, writing – original draft, visualization. Dongyang Li, Jinnuo Hu & Debin Wan: writing – review & editing. Zhen Zhang: resources. Bruce D. Hammock: resources, funding acquisition, supervision.

Conflicts of interest

There are no conflicts to declare.

Acknowledgements

We are very grateful to volunteers for providing samples. We are very grateful to Dr Wan for LC-MS analysis. This work was financially supported by the National Institute of Environmental Health Science Superfund Research Program (P42ES004699) and the National Academy of Sciences and USAID (NAS, Sub-Award No. 2000009144). Any opinions, findings, conclusions, or recommendations expressed in such article are those of the authors alone, and do not necessarily reflect the views of USAID or NAS.

References

1 G. M. Shan, H. Z. Huang, D. W. Stoutamire, S. J. Gee, G. Leng and B. D. Hammock, *Chem. Res. Toxicol.*, 2004, **17**(2), 218–225.
2 D. L. Sudakin, *Clin. Toxicol.*, 2006, **44**(1), 31–37.
3 L. Chen, T. F. Zhao, C. P. Pan, J. H. Ross and R. I. Krieger, *J. Agric. Food Chem.*, 2012, **60**(36), 9342–9351.
4 J. R. Richardson, M. M. Taylor, S. L. Shalat, T. S. Guillot, W. M. Caudle, M. M. Hossain, T. A. Mathews, S. R. Jones, D. A. Cory-Slechta and G. W. Miller, *FASEB J.*, 2015, **29**(5), 1960–1972.
5 K. M. Erstfeld, *Chemosphere*, 1999, **39**(10), 1737–1769.
6 M. Morgan, P. Jones, J. Sobus and D. B. Boyd, *Int. J. Environ. Res. Public Health*, 2016, **13**(11), 1172.
7 Y. Ding, C. A. White, S. Muralidhara, J. V. Bruckner and M. G. Bartlett, *J. Chromatogr. B: Anal. Technol. Biomed. Life Sci.*, 2004, **810**(2), 221–227.
8 A. W. Abu-Qare and M. B. Abou-Donia, *J. Anal. Toxicol.*, 2001, **25**(4), 275–279.
9 M. H. El-Saeid and H. A. Khan, *Int. J. Food Prop.*, 2015, **18**(5), 1119–1127.
10 M. K. Mudiam, A. Chauhan, R. Jain, Y. K. Dhuriya, P. N. Saxena and V. K. Khanna, *J. Chromatogr. B: Anal. Technol. Biomed. Life Sci.*, 2014, **945–946**, 23–30.
11 S. Saito, J. Ueyama, T. Kondo, I. Saito, E. Shibata, M. Gotoh, H. Nomura, S. Wakusawa, K. Nakai and M. Kamijima, *J. Exposure Sci. Environ. Epidemiol.*, 2014, **24**(2), 200–207.
12 I. Bragança, P. C. Lemos, C. Delerue-Matos and V. F. Domingues, *Environ. Sci. Pollut. Res.*, 2019, **26**(3), 2987–2997.
13 M. P. Kavvalakis, M. N. Tzatzarakis, A. K. Alegakis, D. Vynias, A. K. Tsakalof and A. M. Tsatsakis, *Drug Test. Anal.*, 2014, **6**(Suppl 1), 9–16.
14 H. J. Kim, M. R. McCoy, Z. Majkova, J. E. Dechant, S. J. Gee, S. Tabares-da Rosa, G. G. Gonzalez-Sapienza and B. D. Hammock, *Anal. Chem.*, 2012, **84**(2), 1165–1171.
15 S. Thiphom, T. Prapamontol, S. Chantara, A. Mangklabruks, C. Suphavilai, K. C. Ahn, S. J. Gee and B. D. Hammock, *J. Environ. Sci. Health, Part B*, 2014, **49**(1), 15–22.
16 K. C. Ahn, S. J. Gee, H. J. Kim, P. A. Aronov, H. Vega, R. I. Krieger and B. D. Hammock, *Anal. Bioanal. Chem.*, 2011, **401**(4), 1285–1293.

17 J. Q. Huo, Z. F. Li, D. B. Wan, D. Y. Li, M. Qi, B. Barnych, N. Vasylieva, J. L. Zhang and B. D. Hammock, *J. Agric. Food Chem.*, 2018, **66**(43), 11284–11290.
18 A. Y. El-Moghazy, J. Q. Huo, N. Amaly, N. Vasylieva, B. D. Hammock and G. Sun, *ACS Appl. Mater. Interfaces*, 2020, **12**(5), 6159–6168.
19 M. Pali, C. R. S. Bever, N. Vasylieva, B. D. Hammock and I. I. Suni, *Electroanalysis*, 2018, **30**(11), 2653–2659.
20 Y. L. Wang, Z. F. Li, B. Barnych, J. Q. Huo, D. Wan, N. Vasylieva, J. L. Xu, P. Li, B. B. Liu, C. Z. Zhang and B. D. Hammock, *J. Agric. Food Chem.*, 2019, **67**(41), 11536–11541.
21 M. Nichkova, D. Dosev, A. E. Davies, S. J. Gee, I. M. Kennedy and B. D. Hammock, *Anal. Lett.*, 2007, **40**(7), 1423–1433.
22 C. Y. Zhao, Y. Si, B. F. Pan, A. Y. Taha, T. R. Pan and G. Sun, *Talanta*, 2020, **217**, 121054.
23 H. J. Kim, K. C. Ahn, A. González-Techera, G. G. González-Sapienza, S. J. Gee and B. D. Hammock, *Anal. Biochem.*, 2009, **386**(1), 45–52.
24 H. J. Kim, S. J. Gee, Q. X. Li and B. D. Hammock, *ACS Symp. Ser.*, 2007, **966**, 171–185.
25 Y. Lu, N. Xu, Y. Zhang, B. Liu, Y. Song and S. Wang, *Food Agric. Immunol.*, 2010, **21**(1), 27–45.
26 Y. Liu, A. H. Wu, J. Hu, M. M. Lin, M. T. Wen, X. Zhang, C. X. Xu, X. D. Hu, J. F. Zhong, L. X. Jiao, Y. J. Xie, C. Z. Zhang, X. Y. Yu, Y. Liang and X. J. Liu, *Anal. Biochem.*, 2015, **483**, 7–11.
27 C. Hamers-Casterman, T. Atarhouch, S. Muyldermans, G. Robinson, C. Hamers, E. B. Songa, N. Bendahman and R. Hamers, *Nature*, 1993, **363**, 446–448.
28 D. R. Maass, J. Sepulveda, A. Pernthaner and C. B. Shoemaker, *J. Immunol. Methods*, 2008, **324**(1–2), 13–25.
29 L. Liang, Z. X. Hu, Y. Y. Huang, S. L. Duan, J. He, Y. Huang, Y. X. Zhao and X. L. Lu, *J. Nanosci. Nanotechnol.*, 2016, **16**(12), 12099–12111.
30 T. D. Meyer, S. Muyldermans and A. Depicker, *Trends Biotechnol.*, 2014, **32**(5), 263–270.
31 P. Sroga, D. Safronetz and D. R. Stein, *Future Virol.*, 2020, **15**(3), 195–205.
32 Q. Chen, Y. Y. Wang, F. J. Mao, B. C. Su, K. L. Bao, Z. L. Zhang, G. F. Xie and X. Liu, *RSC Adv.*, 2020, **10**(56), 33700–33705.
33 Z. C. Sun, Z. H. Duan, X. Liu, X. Deng and Z. W. Tang, *Food Anal. Methods*, 2017, **10**, 3558–3564.
34 G. Frens, *Nature (London), Phys. Sci.*, 1973, **241**(105), 20–22.
35 S. Thobhani, S. Attree, R. Boyd, N. Kumarswami, J. Noble, M. Szymanski and R. A. Porter, *J. Immunol. Methods*, 2010, **356**(1–2), 60–69.
36 C. Zhang, Y. Zhang and S. Wang, *J. Agric. Food Chem.*, 2006, **54**(7), 2502–2507.